The SPHERE exoplanet imager: Status report at PDR

Francois Wildi[*l], Jean-Luc Beuzit[b], Markus Feldt[c], David Mouillet[b], Kjetil Dohlen[a], Pascal Puget[b], Andrea Baruffolo[d], Julien Charton[b], Jacopo Antichi[d], Pierre Baudoz[e], Anthony Boccaletti[e], Marcel Carbillet[f], Riccardo Claudi[d], Philippe Feautrier[b], Enrico Fedrigo[h], Thierry Fusco[g], Raffaele Gratton[d], Norbert Hubin[h], Markus Kasper[h], Maud Langlois[a], Rainer Lenzen[c], Claire Moutou[a], Alexey Pavlov[c], Cyril Petit[g], Johan Pragt[i], Patrick Rabou[b], Ronald Roelfsema[i], Michel Saisse[a], Hans-Martin Schmid[j], Eric Stadler[b], Christian Thalmann[j],Massimo Turatto[d], Stéphane Udry[1], Rens Waters[k], Thomas Henning[c] , Anne-Marie Lagrange[b] , Farrokh Vakili[f].

[1] Observatoire de Genève, CH-1290 Sauverny, Switzerland
[a] Laboratoire d'Astrophysique de Marseille, B.P. 8, F-13376 Marseille Cedex 12, France
[b] Laboratoire d'Astrophysique de Grenoble, B.P. 53, F-38041 Grenoble Cedex 9, France
[c] Max Planck Institut für Astronomie, Königstuhl 17, D-69117 Heidelberg, Germany
[d] Osservatorio Astronomico di Padova, Vicolo dell'Osservatorio 5, I-35122 Padova, Italy
[e] Laboratoire d'Etudes Spatiales et d'Instrumentation en Astrophysique, F-92190 Meudon, France
[f] Laboratoire Universitaire d'Astrophysique de Nice, Parc Valrose, F-06108 Nice, France
[g] Office National d'Etudes et de Recherches Aérospatiales, B.P. 72, F-92322 Chatillon, France
[h] European Southern Observatory, Karl-Schwarzschild-Strasse 2, D-85748 Garching, Germany
[i] ASTRON, P.O. Box 2, NL-7990 AA Dwingeloo, The Netherlands
[j] Institute of Astronomy, ETH Zurich, CH-8092 Zurich, Switzerland
[k] Universität van Amsterdam, Kruislaan 403, NL-1098 SJ Amsterdam, The Netherlands

ABSTRACT

The SPHERE is an exo-solar planet imager, which goal is to detect giant exo-solar planets in the vicinity of bright stars and to characterize them through spectroscopic and polarimetric observations. It is a complete system with a core made of an extreme-Adaptive Optics (AO) turbulence correction, pupil tracker and interferential coronagraphs. At its back end, an Infra-Red Dual-beam Imaging and Spectroscopy science module and an integral field spectrograph work in the Near Infrared (NIR) Y, J, H and Ks bands (0.95 – 2.32µm) and a high resolution polarization camera covers the visible (0.6 – 0.9 µm) region. We describe briefly the science goals of the instrument and deduce the top-level requirements. This paper presents the system architecture, and reviews each of the main sub-systems. The results of the latest end-to-end simulations are shown and an update of the expected performance is given. The project has been officially kicked-off in March 2006, it is presently undergoing Preliminary Design Review and is scheduled for 1st light in early 2011. This paper reviews the present design of SPHERE but focuses on the changes implemented since this project was presented the last time to this audience[6].

Keywords: extrasolar planets, extreme AO, coronagraph, dual imaging, polarimetry, spectral imaging

1. INTRODUCTION

The SPHERE project (Spectro-Polarimetric High-contrast Exoplanet Research) is the offspring of the two responses to the ESO call for proposals for a VLT planet finder instrument, VLT-PF[1] and CHEOPS[2], embedding the best of each of them. Before and after kick-off our project has undergone a challenging phase of technical and managerial consolidation and it is now well defined and well organized. It is nevertheless a complex system with its extreme AO (SAXO)[3], the coronagraphic devices, and the an Infra-Red Dual-beam Imaging and Spectroscopy science module (IRDIS), its Integral Field Spectrograph (IFS)4 and the ZIMPOL dual imaging polarimeter5. In the following sections a quick reminder of the science case for SPHERE is made. Then the system architecture and its main sub-systems are presented. Finally, we will review the challenges associated with the integration and the operation of such a complex instrument.

1.1. Science case

The prime objective of SPHERE is the discovery and study of new planets orbiting stars by direct imaging of the circumstellar environment. The challenge consists in the very large contrast of luminosity between the star and the planet

[*] François.wildi@obs.unige.ch

(larger than ~12.5 magnitudes or ~10^5 flux ratio), at very small angular separations, typically inside the seeing halo. The whole design of SPHERE is therefore optimized towards high contrast performance in a limited field of view and at short distances from the central star. Both evolved and young planetary systems will be detected, respectively through their reflected light (mostly in the Vis by ZIMPOL) and through the intrinsic planet emission in the NIR (IRDIS and IFS modes). The two NIR imagers will provide complementary detection capacities and characterization potential, in terms of field of view, contrast, and spectral domain.

Current results from direct imaging surveys allow excluding only planet distributions with a large population of massive planets in outer orbits. With its enhanced capabilities (a gain of two orders of magnitudes in contrast with respect to existing instruments) and a list of potential targets including several hundred stars, SPHERE will provide a clear view of the frequency of giant planets in wide orbits. With the number of expected detections (several tens), the level of the large separation wing of the distribution with semi-major axis can probably be estimated with an accuracy of about 20-30%, good enough for a first statistical discussion of the properties of planetary systems.

Imaging of planets already detected by radial velocity and/or astrometry would additionally represent a major breakthrough thanks to the availability of dynamical constraints (or even full orbit determinations) on the planet masses and on the orbital elements. Therefore, these objects will represent the ideal benchmarks for the calibration of models for sub-stellar objects.

Finally, the ZIMPOL polarimetric channel. will be capable to investigate the very nearest stars for the polarization signal from extra-solar planets. There are half a dozen of good candidate systems (α Cen A +B, Sirius, Pricyon, Altair) for which giant planets should be detectable, even if their properties are not ideal (low albedo, not highly polarized, smaller in size than Jupiter). In another handful of targets there is some chance to find high-polarization planets, if they exist around them. Such an instrument will then provide invaluable information with which to hone models in preparation for the Darwin and ELT era. For stars further away a detection of reflected light will be difficult.

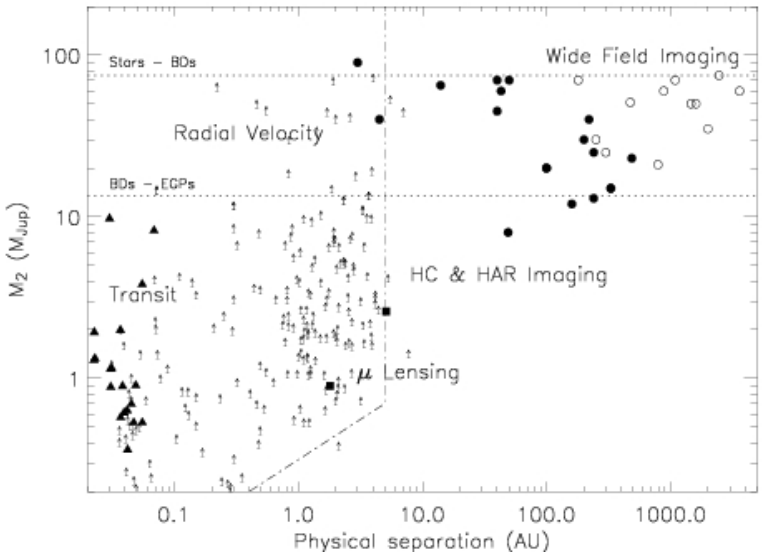

Figure 1. Complementarities between the various detection techniques: radial velocity (arrows), transit (filled triangles), micro lensing (filled boxes), wide field imaging (open circles) and high contrast and high dynamic range imaging (filled circles)

Three main observing modes have been defined in order to draw the maximum benefit of the unique instrumental capabilities of SPHERE. The ***NIR survey mode*** is the main observing mode which will be used for ~80% of the observing time. It combines IRDIS dual band imaging (DBI) in H band with imaging spectroscopy using the IFS in the Y-J bands. This configuration permits to benefit simultaneously from the optimal capacities of both dual imaging over a large field (out to ~5" radius) and spectral imaging in the inner region (out to at least 0.9" radius). In particular, it allows to reduce the number of false alarms and to confirm potential detections obtained in one channel by data from the other channel. This will be a definitive advantage in case of detections very close to the limits of the system.

The ***NIR characterization mode***, in which IRDIS is used alone, will allow observations in Y to short-K, bands in DBI, dual polarimetry, low or medium resolution spectroscopy or in classical imaging. In the ***visible search and characterization mode***, ZIMPOL works alone and offers polarimetric capacities with unique performance in reflected light very close to the star, down to the level required for the first direct detection in the visible of old close-in planets. ZIMPOL also provides classical imaging in the visible, offering unique high-Strehl performance.

2. SYSTEM AND COMMON PATH

2.1. Overview

The architecture of SPHERE has not evolved since it was presented in 2006[1]. It is divided in four subsystems: the Common Path and Infrastructure and the three science instruments IRDIS, IFS, and ZIMPOL. The Common Path includes pupil stabilizing fore optics (tip-tilt and rotation), the SAXO extreme adaptive optics system, a NIR coronagraphic device and a separate visible coronagraphic device. The two NIR instruments (IRDIS and IFS) are fed with the coronagraphed NIR beam and ZIMPOL gets the visible coronagraphed beam, after it has shared the visible photons with the AO wavefront sensor. A photon sharing scheme has been agreed between IRDIS and IFS, allowing IFS to exploit the NIR range up to the J band, leaving the H-band, judged optimal for the DBI mode, for IRDIS during the main observation program. The common path will be mounted on a large actively damped optical bench to which each science instrument will dock as a whole. When in operation on one of the VLT Nasmyth platforms, SPHERE will be capped by a thermal/dust cover. The current design of SPHERE is shown in
Figure 3.
Besides classical optical components, the common path embeds numerous new technology components like the high order deformable mirror, toroidal mirrors manufactured by spherical polishing of pre-stressed substrates, a dedicated electron multiplying CCD for wavefront sensing, achromatic 4 quadrants coronagraph, classical and apodized Lyot coronagraphs. A good number of these components have one or more of their degrees of freedom motorized, for a total of around 60 motors.

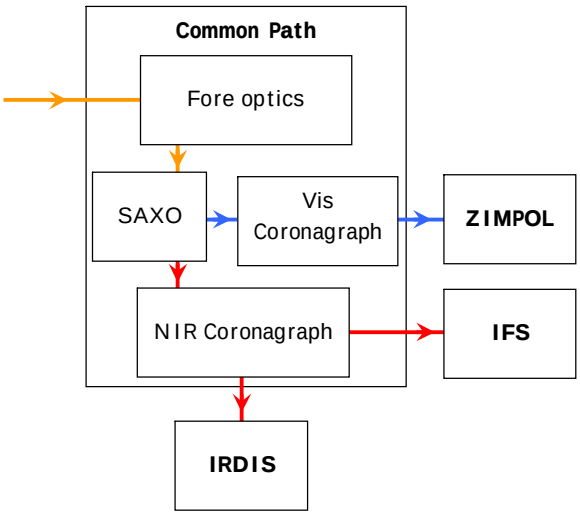

Figure 2. The four sub-systems of SPHERE : Common Path, IRDIS, IFS, and ZIMPOL. Optical beams are indicated in solid for NIR, dotted for Vis and dash/dot for CPI.

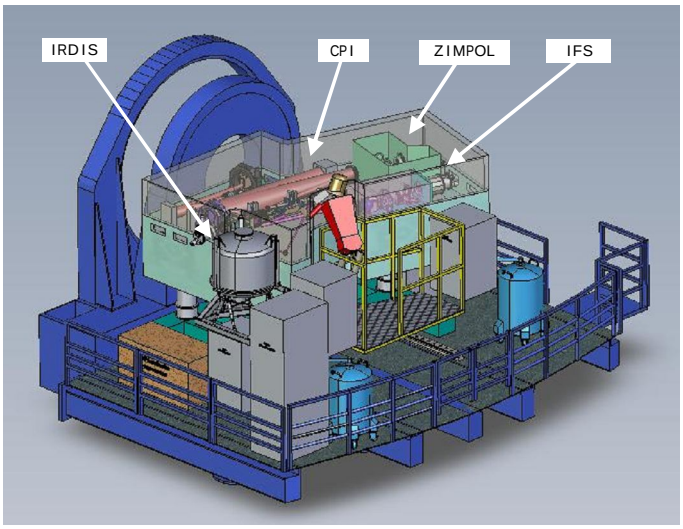

Figure 3. Current opto-mechanical design of SPHERE.

2.2. The SAXO extreme AO system

The SAXO system is composed by 3 loops + one off line calibration

- Main AO loop: correct for atmospheric, telescope and common path defects. The main impact is the increase of detection signal to noise ratio through the reduction of the smooth PSF halo due to turbulence effects.
- The Differential Tip-Tilt loop for fine centering on coronagraph mask (correction of differential tip-tilt between VIS and IR channel). It will ensure an optimal performance of the coronagraph device.
- The Pupil Tip-Tilt loop for pupil shift correction (telescope and instrument). It will ensure that the uncorrected instrumental aberrations effects (in the focal plane) will always be located at the same position and thus will be canceled out by a clever post-processing procedure.
- Non-Common Path Aberrations will be measured with phase diversity, and their pre-compensation will lead to the reduction of persistent speckle[13].

The 41x41 actuator High Order DM of 180 mm diameter has now been manufactured by CILAS and displays a best flat of 5nm rms surface and maximum stroke >±3.5µm (see Figure 4). The high bandwidth (1kHz) tip-tilt mirror (TTM) with ±0.5 mas resolution is being developed by the LESIA in Paris. The wavefront sensor is a 40x40 lenslet Shack-Hartmann, 0.45-0.95µm spectral range equipped with a focal plane spatial filter continuously variable in size from λ/d to 3λ/d at 0.7µm,

where d is the sub-aperture diameter) for aliasing control. It is based on the dedicated 240x240 pixel electron multiplying CCD220 from EEV and will achieve temporal sampling frequency of 1.2 kHz with a read-out-noise < $1e^-$ and a 1.4 excess photon noise factor.
At the heart of the AO system is a Real Time Computer (RTC) Called SPARTA: "Standard Platform for Adaptive optics Real Time Applications", the new generation generic RTC from ESO, providing a global AO loop delay <1 ms. SPARTA allows to control the 3 system loops but it will also provide turbulent parameters and system performance estimation as well all the relevant data for an optimized PSF reconstruction and a clever signal extraction from scientific data.

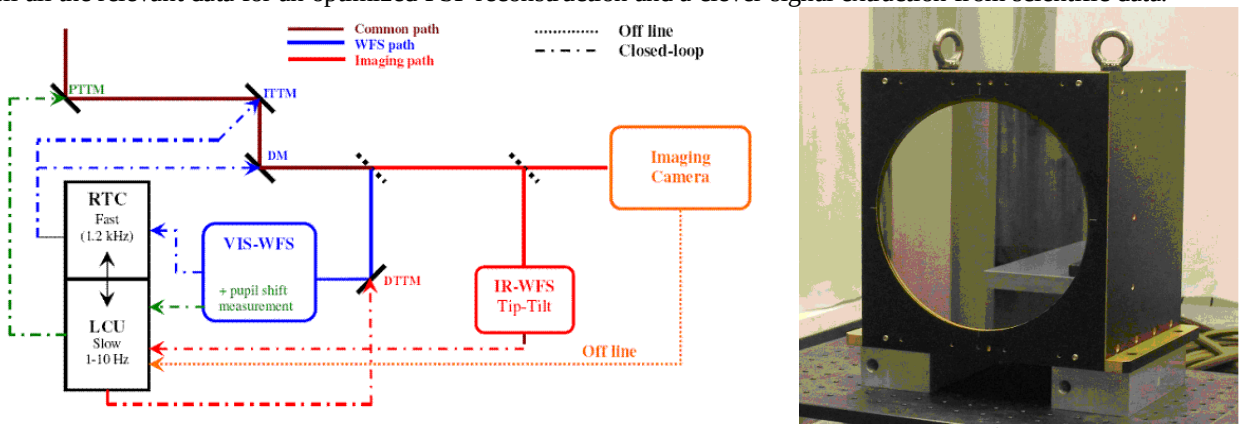

Figure 4. The AO loop structure, with broad-band, NIR and VIS beams in brown, red, and blue resp. The fast (1.2kHz), loop includes the DM, image tip-tilt (ITTM), Vis WFS and RTC. The RTC also generates a slow signal (1-10Hz) for lateral pupil alignment via the pupil tip-tilt mirror (PTTM). Slow differential image motion between the Vis and NIR beams is detected by a NIR sensor, driving a differential tip-tilt plate (DTTP) that will offset the beam on the Vis WFS. The picture shows the finished high order DM.

2.3. Coronagraphs

Coronagraphy is key for reaching our science goals. Its action is to reduce by a factor ≥100 the intensity of the stellar peak, and to eliminate the diffraction features due to the pupil edges. The base-line coronagraph suite will include an achromatic four-quadrant phase mask coronagraph (A4Q) based on precision mounting of four half-wave plates (HWP), and both a classical Lyot coronagraph (CLC) and an apodized Lyot coronagraph (ALC). Other options include the classical four-quadrant phase mask[7] which is now very well mastered and tested in the lab and on the sky with VLT/NACO[8]. More explorative devices are also being investigated options like a broad-band versions[9] of the A4Q based on zero-order gratings or its circularly symmetric version, the annular groove phase mask (AGPM), both fabricated in micro-structured silicon and limited to the H and Ks bands. Because stellar coronagraphy is a quickly evolving field masks are exchangeable at all levels for future improvements.

The A4Q coronagraphs have now been prototyped using the SPHERE f/40 focal and tested in monochromatic and polychromatic light in H, J and Y bands (See Figure 5). In the H band (R = 7) the nulling performance are very similar to that obtained in the monochromatic case at 1.55 µm, indicating the good achromatisation of the component. In the J and Y bands the nulling performance is decreased with a peak-to-peak attenuation of 350 and 315 respectively. However, contrast levels are quite homogeneous with respect to the H band, another indication of reasonable achromatization..

While the CLC option, with mask diameter of about 10λ/D, is within the realm of classical manufacturing, the ALC option requires an apodizer in the coronagraph entrance pupil. Prototyping is ongoing, and a promising technology using graded metal deposition has been identified. An alternative technology based on ion implantation is also considered, but this technology gives discrete steps in the apodization profile. The effects of this are being quantified by simulations.

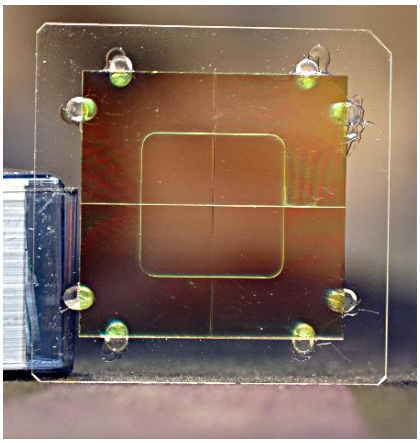

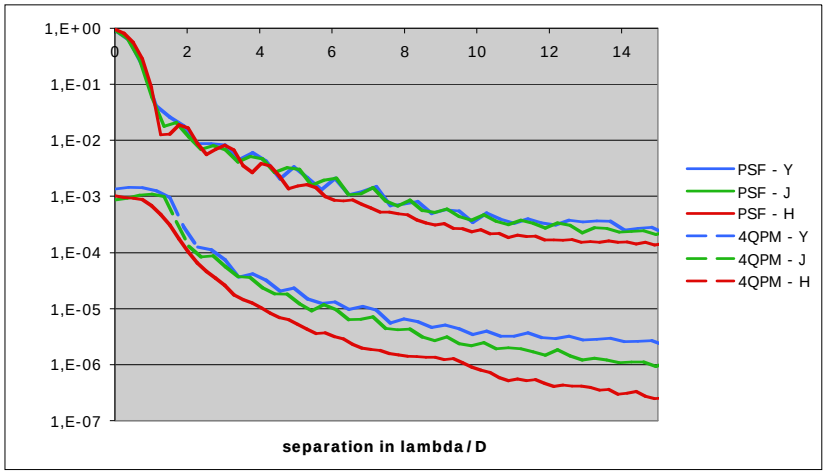

Figure 5. SPHERE A4Q focal plane mask prototype. The left picture shows the complete assembled device (tungsten wires are placed to mask the edges of the wave plates). Right graph shows radial contrast in Y, J and H. The X axis is scaled to each wavelength.

3. IRDIS

3.1. Overview

The Infra-Red Dual-beam Imaging and Spectroscopy (IRDIS) science module covers a spectral range from 950-2320 nm with an image scale of 12.25mas consistent with Nyquist sampling at 950nm. The FOV is 11" x 12.5", both for direct and dual imaging. Dual band imaging (DBI) is the main mode of IRDIS, providing images in two neighboring spectral channels with <10nm rms differential aberrations. Two parallel images are projected onto the same 2kx2k detector with 18µm square pixels, of which they occupy about half the available area. A series of filter couples is defined corresponding to different spectral features in modeled exoplanet spectra. The classical imaging (CI) mode allows high-resolution coronagraphic imaging of the circumstellar environment through broad, medium and narrow-band filters throughout the NIR bands including Ks. In addition to these modes, long-slit spectroscopy (LSS) at resolving powers of 50 and 500 is provided, as well as a dual polarimetric imaging (DPI) mode. A pupil-imaging mode for system diagnosis is also implemented.

All these modes require a coronagraph in the common path system and a corresponding Lyot stop in the IRDIS Lyot stop wheel. For the Long Slit Spectroscopy mode, the coronagraph mask is replaced by a coronagraphic slit. The slit is centered on the star, which is covered by a central patch, and a disperser device equipped with a dedicated Lyot stop is located in the IRDIS Lyot stop wheel. Two dispersion devices are provided, a double prism (same concept as in CONICA) for low resolution (LRS, ~50) and a grism for medium resolution (MRS, ~500). The prism can be used with either a YJHKs filter or a YJH filter, and the grism is used only with the YJH filter.

The main challenge of IRDIS is to achieve less than 10nm differential aberrations between the two channels. An error budget based on high-quality polishing technology is found to satisfy the requirement, and prototyping of DBI filters confirms this budget. The beam-splitter option has been favored over the alternative Wollaston-based option because it eliminates spectral blurring problems, which would limit the useful FOV, and allows the use of high-quality materials with high homogeneity.

The current opto-mechanical design of the IRDIS optical bench is shown in Figure 6 (a). The entrance pupil coincides with the coronagraphic exit pupil (Lyot stop). Located in a collimated beam of diameter 10mm, it constitutes the main optical interface with the common path optics. Beam splitter and imaging optics is located in a compact unit, allowing minimal thermal gradients and optimal mechanical stability. Three wheels are provided within the cryogenic environment; see Figure 6 (a). In order to limit the overhead in case of motor failure, the motors are mounted outside of the cold screen so as to be accessible without dismounting the bench. However, to simplify the overall design, they are kept within the cryostat. Motor replacement therefore requires breaking the thermal vacuum, but does not require re-alignment of the instrument, limiting such interventions to below 5 days as required by ESO. The detector is mounted on a two axis translation stage to allow dithering for flat-field improvement. This stage, whose development is based on CONICA heritage, is powered by PI piezo motors, currently undergoing cryogenic qualification.

The cryostat concept is shown in Figure 6 (b).Cooling power is provided by two liquid nitrogen tanks with capacity for 30h autonomy. The detector will be kept at ~80K, and the optics is stabilized at a temperature below 150K to limit thermal background. The interface with the common path bench is ensured via a bracket fixed on the side of the table. IRDIS is fixed to this bracket via a hexapod structure which is very stiff and allows six degrees of freedom for position adjustment.

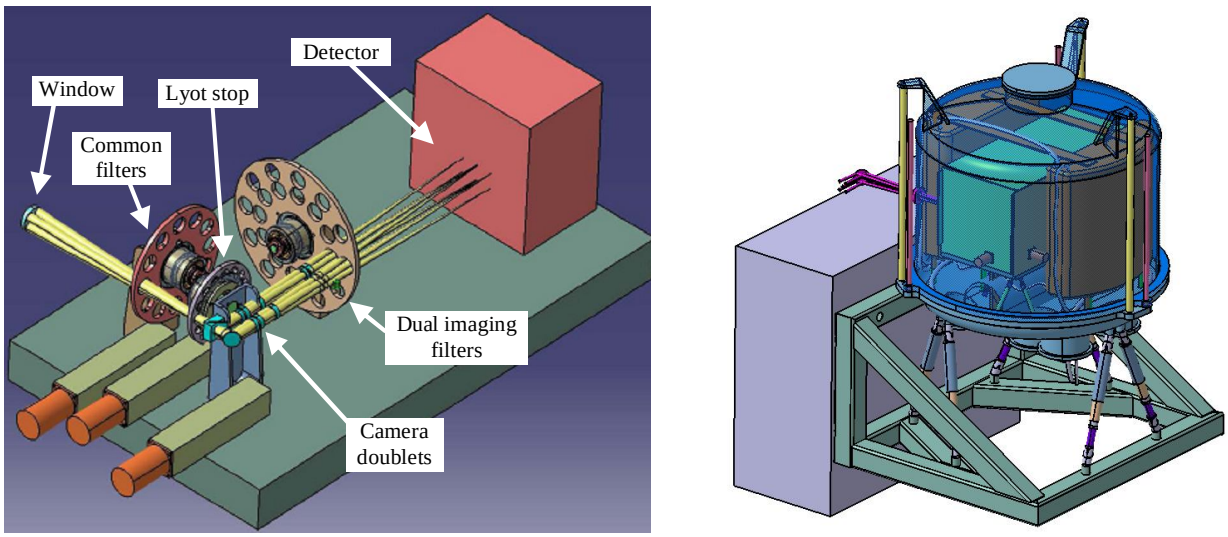

(a) (b)

Figure 6. View of the IRDIS optical bench (a) and cryostat (b).

3.2. Dual-band imaging performance

Numerical simulations of the IRDIS performance have been made along the lines described in Ref 6, using the versatile CAOS platform[12]. Typical simulated DBI images are shown in Figure 7. For this mode, the Top Level Requirement is a 5σ contrast of 5 10^{-5} at 0.1" and 5 10^{-6} at 0.5" from the star in 1hour integrations achieved by imagery at both sides of the H-band methane absorption edge.

High contrast imaging has to deal at first order, with two components: a speckled halo which is averaging over time and a static speckle pattern originating from quasi-static aberrations evolving occurring with a much longer lifetime than atmospheric residuals. Because the DBI mode is performing simultaneous differential imaging, Performances are mostly limited by the quasi-static aberrations upstream the coronagraph and by the spectral separation between DBI filters. Smaller differential aberrations are not necessary unless spectral separation is made smaller in the same ratio. However, spectral separation is here imposed by the spectral characteristics of the planets to be observed and therefore cannot be reduced..

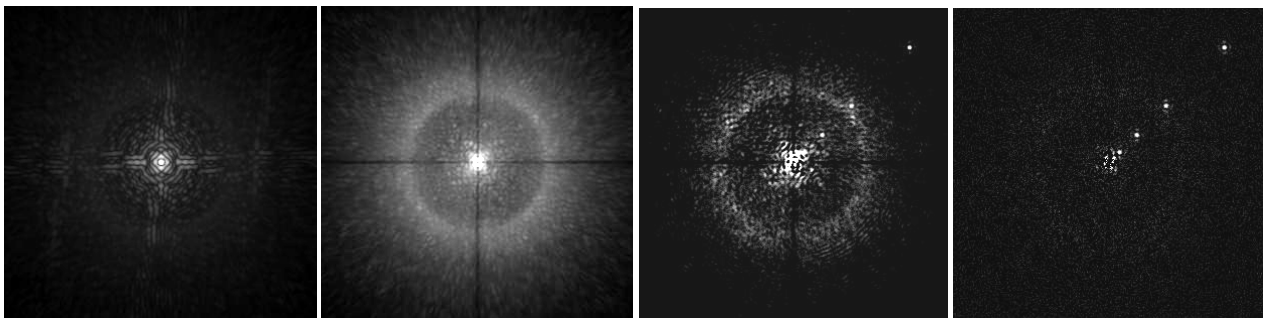

(a) (b) (c) (d)

Figure 7: M0V star 10pc image with DBI (H2H3), the detected planets are located at 0.1", 0.2", 0.5", 1", 2" from the star and correspond to : 1MJ at 10My - 3MJ at 100My - 11MJ at 1Gy - 25MJ at 5Gy. The illustrations show the star PSF (a), the 4QPM raw image (b), the 4QPM single subtraction of 2 wavelengths H2H3 (c), the double subtraction image including calibration of differential aberrations and chromatic residual (d). Gray scales are arbitrary.

3.3. Long-slit spectroscopy performance

An efficient method for data reduction of the slit spectroscopy mode is illustrated. The final goal is to extract the spectra of the companions from that of the star by removing the speckled contributions of the star that form oblique lines in the spectrum.

First, the spectral image is over-sampled and spatially rescaled so that speckles form horizontal lines in the spectrum (Sparks & Ford 2002), see Figure 8 (a, b). Second, a large number of lines are averaged in order to obtain the spectrum of the star. The presence of a companion signal is not critical as long as its contribution is small. This spectrum, multiplied by an ad-hoc constant, is subtracted from each line, leaving a residual random noise together with the companion signal, see

Figure 8 (c). The last step is to spatially scale the spectrum back to its original scale, so that the companion spectrum reappears on a straight line, see Figure 8 (d). It is then possible to extract the companion spectra for analysis. The final result can be improved by using a reference star, in the same way that a reference star is used in DBI mode, for the double subtraction. Then, a part of speckle residues common to the star and the reference, especially close to the star where speckles are not very well removed by the interpolation, are further attenuated, see Figure 8 (e).
The LSS achieves slightly better performances than DBI mainly because the fitting of the speckles over a large wavelength range. Also, there is no differential aberrations because the LSS image forms one image on one IRDIS Channel and the chromatic aberrations in a given channel are very small (WFE < 1 nm between 2 pixels).

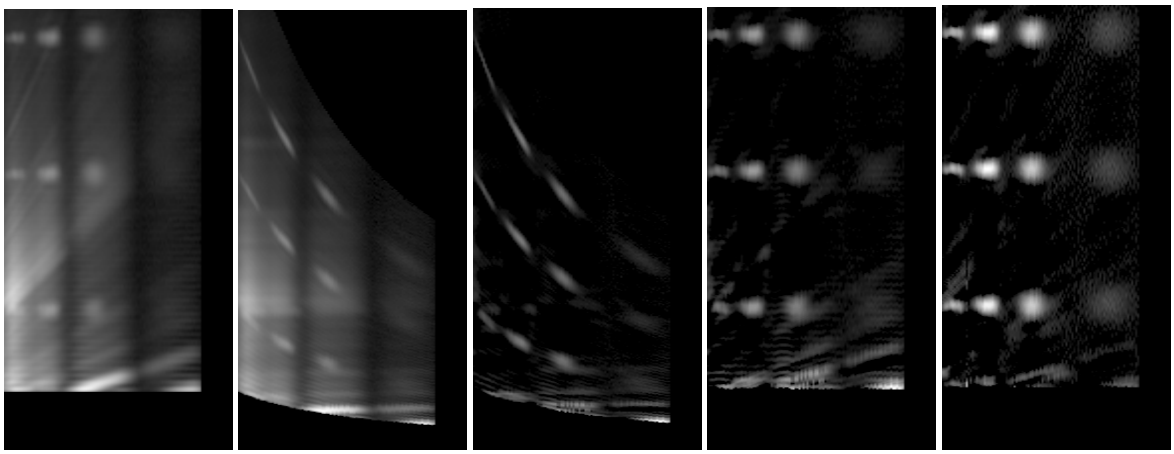

(a) (b) (c) (d) (e)

Figure 8: Over-sampled (a) and spatially rescaled (b) spectral image. Spectrum on which the linear spectrum of the star has been subtracted on each line (c), and rescaled to its original spatial scale to bring back the companion spectrum on a straight line (d). Reduced spectral image including reference subtraction (e). Gray scales are arbitrary.

In low-resolution spectroscopy (LRS), we will be able to characterize both objects detected by SPHERE in the NIR survey mode, and companions of stars already known in the literature, providing they are within the field of view of IRDIS. With a simple Lyot occulting mask in the centre of the field, and limited contrast in the vicinity of the star, the angular separations (>0.5'') will be within access to this mode. The simulation show that we should obtain a signal-to-noise ratio of 20 or larger for a 700K-1000K companion around a typical target of SPHERE (e.g. around a H=6 magnitude star at less than 50 pc) allowing characterization of the J-Ks color of cool planets.
The MRS Medium Resolution mode also allows observations in the full 11 arcsec field-of view, except the central part which is occulted by the coronograph. The scientific exploitation of these data is based on the observation of molecular and atomic bands that are sensitive to the temperature and gravity, and require a resolution of at least 400. The performed simulation show that the gravity-sensitive KI feature is clearly resolved for moderate companions temperature (> 900K) and separation larger than 0.5" with signal to noise ratio > 20 for both G0 and M0 star at 10pc.

4. IFS

IFS's are very versatile instruments, well adapted for spectroscopic differential imaging as needed for detection of planets around nearby stars. The main advantage of IFS's is that differential aberrations can be kept at a very low level; this is true in particular for lenslet based systems, where the optical paths of light of different wavelength within the IFS itself can be extremely close to each other. Additionally, an IFS provides wide flexibility in the selection of the wavelength channels for differential imaging, and the possibility to perform spectral subtraction, which in principle allows to recover full information on the planet spectra, and not simply the residual of channel subtraction, as in classical differential imagers[14]. The main drawback of IFS's is that they require a large number of detector pixels, resulting in a limitation in the field of view, which is more severe for lenslet based systems. Classical differential imagers and IFS's are then clearly complementary in their properties, and an instrument where both these science modules are available may be extremely powerful for planet search.

Both a classical TIGER[10,11] and an innovative BIGRE[6] concept have been considered for the SPHERE IFS, the latter being finally selected because of its better properties. Both these designs are based on lenslet systems: in the case of TIGER design the array of micropupil images created by the lenslet array are imaged on the detector, after having being dispersed; in the case of the BIGRE array, a second lenslet array allows formation of pseudo-slit images corresponding to a very small portion of the field, which are then imaged on the detector after being dispersed. The main advantage of the BIGRE

concept is that the pseudo-slit images are only very mildly dependent on wavelength and have a quasi-top-hat profile, while in the TIGRE concept the micropupil images are diffraction images with secondary maxima, whose size is dependent not only on wavelength, but also on the illumination of the individual lenslets. The BIGRE system allows a better control of diffraction effects and a much lower level of cross-talk. Achievement of specifications of the BIGRE concept, was proven with a laboratory prototype at INAF-OAPD.

The 5-σ detectivity at 0.5" is from 10^{-6} to 10^{-7} with respect to the un-occulted PSF peak, depending on star and observing conditions (and on definition: monochromatic vs broad band), and the spectral range of the IFS is limited to the Y-J bands (0.95-1.35μm; an extension to the H band is under study), allowing the use of a single detection channel and parallel operation of IRDIS and IFS. A resolving power per pixel of ~100 is obtained, with a 1.77" (side) square FOV. Nyquist-limited spatial sampling at 0.95μm is imposed as for IRDIS. Optimized commonality between IFS and IRDIS in terms of detector and associated equipment is seen as an important system goal. The same 2kx2k detector format is therefore adopted, and the long-wavelength cut off defined for IRDIS is also acceptable for IFS.

In addition to the micro-lens system at the entrance of the spectrograph, the opto-mechanical concept includes collimation optics, an Amici Prism providing zero beam deviation and constant resolution within the entire wavelength range, camera optics, and the detector cryostat, see Figure 9 (left). Thermal background is controlled by extending the cryostat >150mm in front of the detector, thus limiting the solid angular view of the warm environment, and by including a cold short-pass filter. Detector dithering (in order to improve flat-field precision) is achieved by small movements of the camera optics, realized by commercial piezo's.

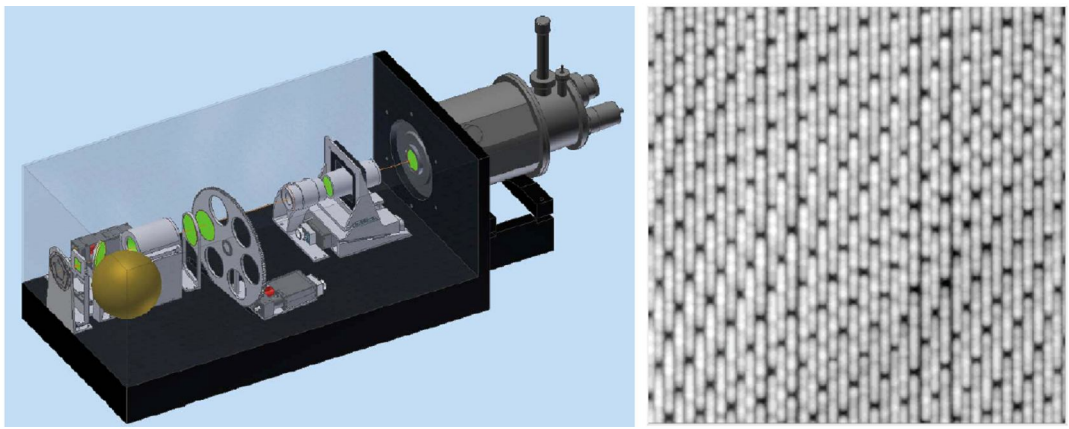

Figure 9. Opto-mechanical design of the IFS (left) and a portion of a simulated detector image (right).

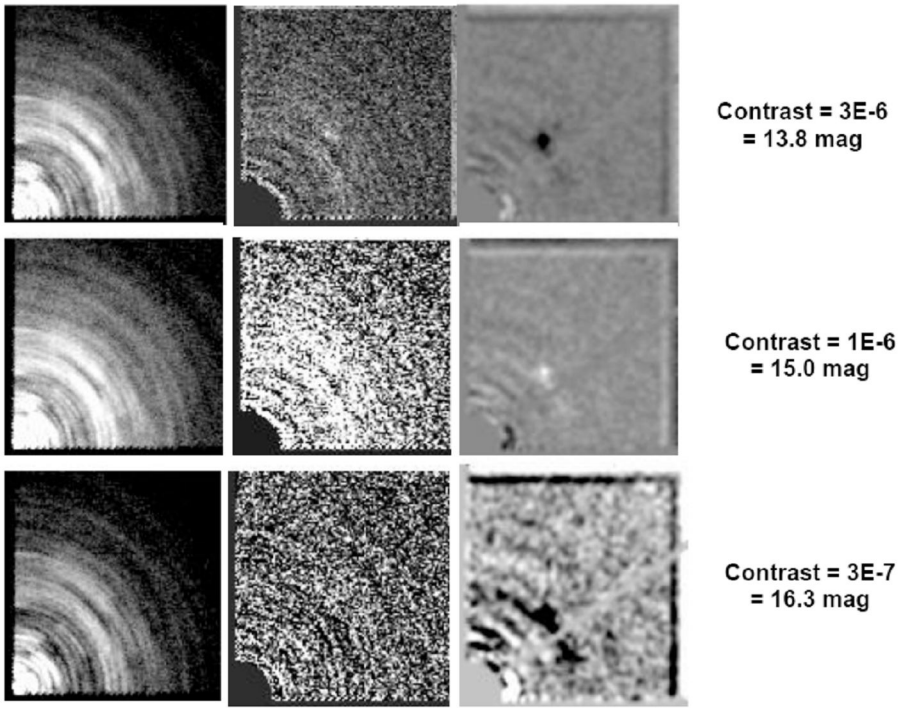

Figure 10. Examples of images extracted from simulations. Top row: on the left: monochromatic image. The planet is at 0.5 arcsec from a G2V star at 10 pc and has a contrast of 3E-06, and it is not clearly visible in the image. Top row, center: single difference image for the same case, made using a pair of wavelengths where the planet signal is present/absent; the planet is barely detected at low S/N (however, above the threshold of S/N=5). Top row on the right: image obtained combining all wavelengths, following an appropriate mask approach. The planet (in this case appearing as a dark spot) is now very obvious. Central row: same case but with a contrast of 1E-06. The planet (this time a bright spot) is clearly visible only on the image obtained with a mask approach. Bottom row: same case but with a contrast of 3E-07. The planet is barely visible only on images obtained with the mask approach.

Examples of simulations of the SPHERE-IFS output are given in Figure 10. Sensitivity is mainly limited by common path static aberrations; since these are expected to be essentially stable with respect to the pupil, sensitivity may be increased by exploiting the rotation of the field with respect to the pupil. The examples we show are for a 30 degree pupil rotation, which is typical for exposures of about 1 hr.

5. ZIMPOL

ZIMPOL (Zurich Imaging Polarimeter) is located behind SPHERE's visible coronagraph. Among its main specifications are a bandwidth of 600 to 900 nm (with a goal of 500 to 900 nm) and an instantaneous field of view of 3 x 3 arcsec^2 with access to a total field of view of 8 arcsec diameter by an internal field selector. The ZIMPOL optical train contains a common optical path that is split with the aid of a polarizing beamsplitter in two optical arms. Each arm has its own detector. The common path contains common components for both arms like calibration components, common filters, a rotatable half wave plate and a ferroelectric liquid crystal polarization modulator. The two arms have the ability to measure simultaneously the two complementary polarization states in the same or in distinct filters. The images on both ZIMPOL detectors are Nyquist sampled at 600 nm. The detectors are both located in the same cryostat and cooled to -80^{o}C. The rest of the ZIMPOL opto-mechanical system is at ambient temperature.

The basic ZIMPOL principle for high-precision polarization measurements includes a fast polarization modulator with a modulation frequency in the kHz range, combined with an imaging photometer which demodulates the intensity signal in synchronism with the polarization modulation. The polarization modulator and the associated polarizer convert the degree-of-polarization signal into a fractional modulation of the intensity signal, which is then measured in a demodulating detector system by a differential intensity measurement between the two modulator states. Each active pixel measures both the high and the low states of the intensity modulation and dividing the differential signal by the average signal eliminates essentially all gain changes, notably changes of atmospheric transparency or electronic gain drifts.

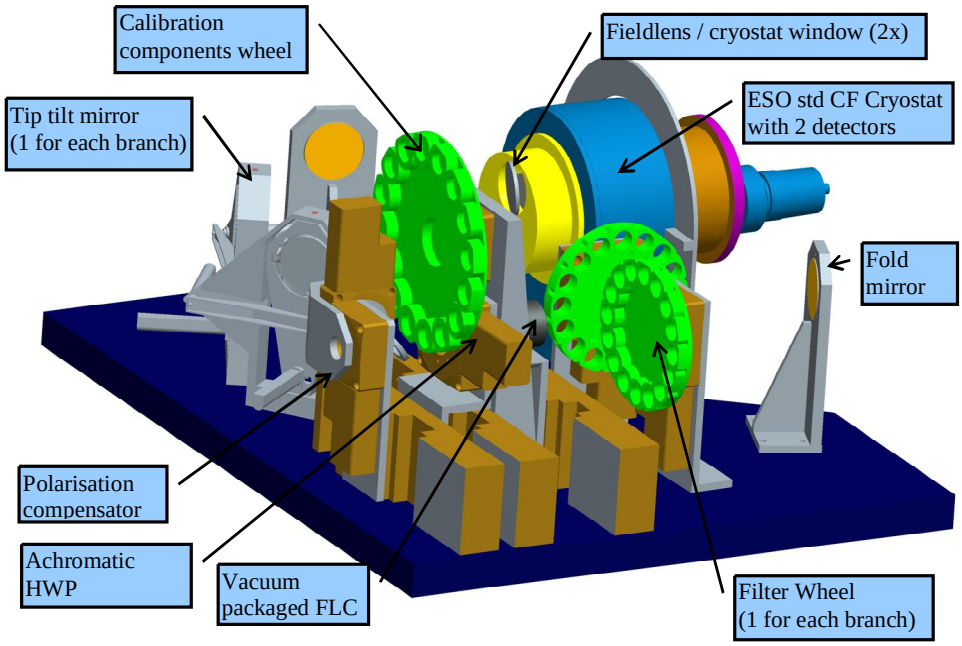

Figures 11 . ZIMPOL Opto-mechanical design

In ZIMPOL/SPHERE the modulator is a ferroelectric liquid crystal (FLC) working at a frequency of about 1 kHz. The demodulator is a special ZIMPOL CCD camera which measures for each active pixel the intensity difference between the two modulation states. For this every second row of the CCD is masked so that charge packages created in the unmasked row during one half of the modulation cycle are shifted for the second half of the cycle to the next masked row, which is used as temporary buffer storage (the CCD can be equipped with cylindrical micro-lenses which focus the light onto the open CCD rows). After many thousands of modulation periods the CCD is read out within less than one second. The sum of the two images is proportional to the intensity while the normalized difference is the polarization degree of one Stokes component. Because the measurement is fully differential, systematic error sources are reduced to a very low level (on the order 10^{-5}). The main requirement is, that the incoming signal is not strongly polarized ($p<10^{-2}$).

The main points of the ZIMPOL specification, deduced from the SPHERE science case, are summarized below:
ZIMPOL shall provide an imaging polarimeter / imager based on the ZIMPOL principle

- With a polarimetric sensitivity of 10^{-5} in the PSF halo (>0.15 aresec) of bright stars
- With an absolute polarimetric accuracy of $< 10^{-3}$
- wavelength range 600-900nm (goal: 500-900nm)
- detector FoV of 3 x 3 arcsec (full field size accessible is 4 arcsec in radius)
- With a set (>10) of filters
- coronagraphic and non-coronagraphic modes

5.1. Performance analysis

The faint polarization signal of the planet has to be extracted from the strong PSF speckle halo of the central star. For this it can be assumed that the polarization measuring sensitivity of 10^{-5} can be achieved as demonstrated in lab experiments. However, a major obstacle is the residual speckle noise pattern in the polarization image due mainly to suspected differential aberrations in the FLC polarization modulator. This residual speckle noise can be further reduced by polarization switching at the entrance of SPHERE, causing the polarization signal from the sky to be inverted, while instrumental effects remain similar. Subtracting the two switched images will strongly reduce the speckle residue. Angular differential imaging is an additional means to average down any remaining noise pattern. This is illustrated in Figure 12**,** showing the results of a simulation with several strongly polarized (50%) planets around a G0V star at a distance of 3 pc.

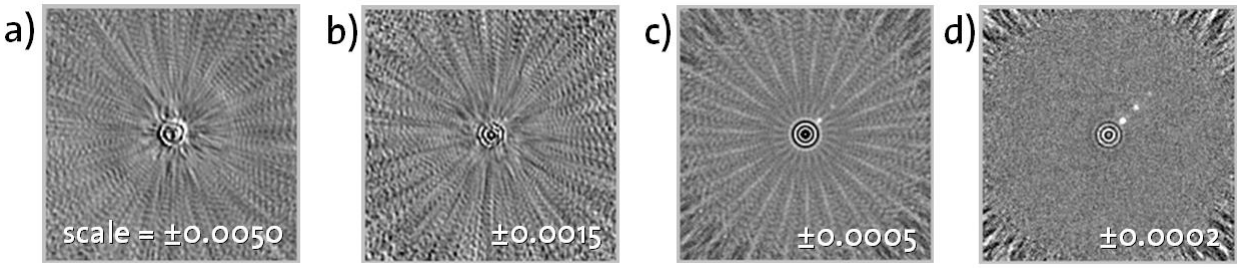

Figure 12: Differential images of a G0V star at 3pc with three orbiting planets at different stages of data reduction. Panel a) the raw polarization image of the coronagraphic PSF, b) the same after calibration with the switched-signal measurement, c) the same after angular averaging using 23 steps of active field rotation, and d) the same after perfect angular differential imaging (subtraction of the background not co-rotating with the field). The detectivity is limited by photon noise in this idealized case. Gray scales are arbitrary.

6. CALIBRATION, DATA REDUCTION AND HANDLING

SPHERE is a highly specialized instrument which stretches the control of technical tolerances to the limits both during the design and manufacturing phases, and particularly during its many extensive calibration procedures. It is clear, that with such an instrument the greatest care must be taken to ensure that quality of the data taken at the telescope indeed matches the excellence of the instrument itself.

This is why it was decided that SPHERE needs a rather unique ``Data Reduction and Handling" (DRH) software package which accompanies the data from the state of observation preparation -- i.e. optimizing target lists, preparing and scheduling observations and calibrations, via the reduction of raw date as they come from the instrument's detectors, to the analysis and search for planetary signals and the final inclusion of detected candidates in the target lists and the scheduling of follow-up observations.

Specifically during the reduction of both calibration and science data, strict error propagation control is designed into the DRH software in order to enable sophisticated analysis and planet signal search by modelling all instrumental and atmospheric properties. Indeed, SPHERE will be the first instrument at ESO, the data pipelines of which not only deliver nice-to-look-at data for home analysis, but also pipelines that run high-fidelity signal searches and deliver all found planetary candidates for all SPHERE data sets taken by any user. This will ensure a homogenous quality of (non-)detections achieved with SPHERE and enables re-processing of all data when improved versions of the analysis routines become available.

7. CONCLUSION

We have presented here the status of SPHERE, exactly at the time of it preliminary design review. Development and prototyping of keystone elements has been successful and all top level requirements are expected to be met. With the final HODM being manufactured and the real time controller forging ahead, the AO system is taking shape. Thanks to a substantial simulation effort, performance budgets are available for each of the focal plane sub-systems. The complex team involving a large consortium of European institutes is now well honed and efficient but the leadership of such a complex instrument remains challenging in terms of technical budgets, resource management and interface control and integration.

ACKNOWLEDGEMENTS

SPHERE is an instrument designed and built by a consortium consisting of LAOG, MPIA, LAM, LESIA, LUAN, INAF, Observatoire de Genève, ETH Zurich, NOVA, ONERA and ASTRON in collaboration with ESO.

REFERENCES

1. Mouillet, D.; Lagrange, A. M.; Beuzit, J.-L.; Moutou, C.; Saisse, M.; Ferrari, M.; Fusco, T.; Boccaletti, A., "High Contrast Imaging from the Ground: VLT/Planet Finder," in *Extrasolar Planets: Today and Tomorrow*, Jean-Philippe Beaulieu, Alain Lecavelier des Etangs and Caroline Terquem (eds), ASP Conf. Proc. 321, 2004, p.39.
2. M. Feldt, T. Henning, S. Hippler, M. Turatto, R. Neuhaeuser, H. M. Schmid, R. Waters "The CHEOPS project: CHaracterizing Exo-planets by Opto-infrared Polarimetry and Spectroscopy" in *Exploring the cosmic frontiers: Astrophysical instruments for the 21st century*, Proc. ESO Astrophysics Symposium (2005).
3. T. Fusco, C. Petit, J.-F. Sauvage, G. Rousset, M. Kasper, K. Dohlen, J. Charton, P. Rabou, P. Feautrier, P. Baudoz, J.-L. Beuzit, M. Downing, E. Fedrigo, D .Mouillet, P. Puget, "Design of the extreme AO system for the planet-finder instrument of the VLT," in *Advances in Adaptive Optics II*, Brent L. Ellerbroek, Domenico Bonaccini, eds, Proc. SPIE 6272 (2006).
4. R.U. Claudi, M. Turatto, J. Antichi, R. Gratton, S. Scuderi, E. Cascone, D. Mesa, S. Desidera, A. Baruffolo, A. Berton, P. Bagnara, E. Giro, P. Bruno, D. Fantine, J.-L. Beuzit , P. Puget, K. Dohlen. "The Integral Field Spectrograph of

SPHERE: the Planet Finder for VLT." in: *Ground-based and Airborne Instrumentation for Astronomy*, Ian S. McLean, Masanori Iye, eds, Proc SPIE 6269 (2006)

5. D. Gisler, H.M. Schmid, C. Thalmann, H.P. Povel, J.O. Stenflo, F. Joos, M. Feldt, R. Lenzen, J. Tinbergen, R. Gratton, R. Stuik, D.M. Stam, W. Brandner, S. Hippler, M. Turatto, R. Neuhauser, C. Dominik, A. Hatzes, Th. Henning, J. Lima, A. Quirrenbach, L.B.F.M. Waters, G. Wuchterl, H. Zinnecker, "CHEOPS/ZIMPOL: a VLT instrument study for the polarimetric search of scattered light from extrasolar planets," in: ``Ground-based instrumentation for astronomy", A.F.M. Moorwood & M. Iye (eds.), SPIE Conf. Vol. 5492, 463-474 (2004)
6. K. Dohlen; J.-L. Beuzit; M. Feldt; D. Mouillet; P. Puget; J. Antichi; A. Baruffolo; P. Baudoz; A. Berton; A. Boccaletti; M. Carbillet; J. Charton; R. Claudi; M. Downing; Ch. Fabron; Ph. Feautrier; E. Fedrigo; T. Fusco; J.-L. Gach; R. Gratton; N. Hubin; M. Kasper; M. Langlois; A. Longmore; C. Moutou; C. Petit; J. Pragt; P. Rabou; G. Rousset; M. Saisse; H.–M. Schmid; E. Stadler; D. Stamm; M. Turatto; R. Waters; F. Wildi, "SPHERE: A planet finder instrument for the VLT" in: *Ground-based and Airborne Instrumentation for Astronomy*, Ian S. McLean, Masanori Iye, eds, Proc SPIE 6269 (2006).
7. Rouan, D.; Riaud, P.; Boccaletti, A.; Clénet, Y.; Labeyrie, A., "The Four-Quadrant Phase-Mask Coronagraph. I. Principle," PASP 112, pp. 1479-1486 (2000).
8. Boccaletti, A.; Riaud, P.; Baudoz, P.; Baudrand, J.; Rouan, D.; Gratadour, D.; Lacombe, F.; Lagrange, A.-M., "The Four-Quadrant Phase Mask Coronagraph. IV. First Light at the Very Large Telescope," PASP 116, pp. 1061-1071 (2004).
9. Mawet, Dimitri; Riaud, Pierre, "Subwavelength gratings for phase mask coronagraphy: the 4QZOG and AGPM coronagraphs," In: *Direct Imaging of Exoplanets: Science & Techniques*, C. Aime and F. Vakili (eds). Proc. IAU 200, Cambridge (2006), pp.361-366.
10. Bacon, R.; Adam, G.; Baranne, A.; Courtès, G.; Dubet, D.; Dubois, J.-P.; Georgelin, Y.; Monnet, G.; Pecontal, E.; Urios, J., "The Integral Field Spectrograph TIGER," in: *Proceedings of ESO Conference on Very Large Telescopes and their Instrumentation*, Marie-Helene Ulrich (ed.), ESO 1988, p.1185.
11. Bacon, R, "The integral field spectrograph TIGER: results and prospects. In: *3D Optical Spectroscopy Methods in Astronomy*, G. Comte, M. Marcelin (eds), ASP Conf. Series 71, 1995, p. 239
12. Carbillet, M.; Verinaud, Ch.; Guarracino, M.; Fini, L.; Lardiere, O.; Le Roux, B.; Puglisi, A. T.; Femenia, B.; Riccardi, A.; Anconelli, B.; Correia, S.; Bertero, M.; Boccacci, P., "CAOS: a numerical simulation tool for astronomical adaptive optics (and beyond)," In: *Advancements in Adaptive Optics*. Proc. SPIE 5490, pp. 637-648 (2004).
13. A. Blanc, T. Fusco, M. Hartung, L. M. Mugnier et G. Rousset, "Calibration of NAOS and CONICA static aberrations. Application of the phase diversity technique," Astron. Astrophys., 399 (2003), pp. 373–383.
14. Thatte, N., Abuter, R., Tecza, M., Nielsen, E.L., Clarke, F.J., Close, L.M., 2007, MNRAS, 378, 1229, "Very high contrast integral field spectroscopy of AB Doradus C: 9-mag contrast at 0.2arcsec without a coronagraph using spectral deconvolution"